

Absolute spectral gaps for infrared light and hypersound in three-dimensional metallodielectric phoxonic crystals

N. Papanikolaou,^{1,a)} I. E. Psarobas,¹ and N. Stefanou²

¹*Institute of Microelectronics, NCSR "Demokritos," GR-153 10 Athens, Greece*

²*Section of Solid State Physics, University of Athens, Panepistimioupolis, GR-157 84 Athens, Greece*

(Received 17 February 2010; accepted 23 May 2010; published online 11 June 2010)

By means of full electrodynamic and elastodynamic multiple-scattering calculations we study the optical and acoustic properties of three-dimensional lattices of metallic nanospheres implanted in a dielectric host. Our results show that such structures exhibit omnidirectional spectral gaps for both telecom infrared light and hypersound, with relatively low absorptive losses. This class of dual (phoxonic) band-gap materials is an essential step toward the hypersonic modulation of light and could lead to the development of efficient acousto-optical devices. © 2010 American Institute of Physics. [doi:10.1063/1.3453448]

The study of the propagation of waves in inhomogeneous media is a problem of wide interest because of its implications in technology and the broad view that can provide in understanding a large area of physical problems.¹ In particular, classical wave transport in periodic media can provide the means to control light, sound or both with the development of so-called classical spectral gap materials. One of the most important properties of such materials is the existence of frequency regions, the so-called band gaps, where propagation is not allowed and all waves are decaying. Such effects are established for both electromagnetic (EM) (Refs. 2 and 3) and acoustic^{4,5} fields. Photonic crystals with submicron periodicity have band gaps in the visible and near infrared part of the spectrum promising applications in optical sensors and telecommunications. Phononic crystals on the other hand are mainly studied in more macroscopic length scales in the order of millimeter. Only very recently, elastic composites with submicron periodicity were demonstrated with acoustic band gaps in the gigahertz range.^{6,7} Tailoring both acoustic and optical properties on the same system can lead to applications which require better control of the acousto-optic interaction.⁸ It was proposed that phoxonic crystals having dual spectral gaps for both photons and phonons could lead to promising applications.⁹

Photonic crystals are likely to act also as phononic crystals. For example, vibrational modes confined in nanoparticles can be excited by a short optical pulse and observed as modulations of the transient reflectivity or transmission on a picosecond time scale. This was reported in a study of coherent vibrations of submicron spherical gold shells in a photonic crystal.¹⁰ It has also been demonstrated, in opals of silica nanospheres, that light can be modulated by acoustic waves.¹¹ However it is well known¹² that absolute band gaps are rather hard to achieve with low-refractive-index dielectric spheres, so silica opals show only directional gaps. Very recently, simultaneous localization of light and sound as well as generation of ultrasound using light was achieved on a patterned Si nanostripe^{13,14} capable of colocalizing and strongly coupling 200 THz photons and 2 GHz phonons. The observed results were attributed to optomechanical coupling which is an elastic vibration due to increased radiation

pressure of the confined light in a carefully designed optomechanical cavity. These results indicate that elastic and EM fields can be made to interact in a controlled manner inside cavities and, toward this end, structures with absolute photonic and phononic band gaps are needed. Recently, such dual band gaps have been reported on two-dimensional (2D) structures of cylindrical holes in LiNbO₃.¹⁵

It has been shown that 2D solid-fluid periodic structures can very easily support dual complete band gaps¹⁶ and, by introducing point defects,¹⁷ one can obtain localized photonic and phononic modes inside the gaps. As a result, Maldovan *et al.*¹⁷ predict that such structures can integrate the management of sound, heat, and light. Nevertheless, the task of constructing three-dimensional (3D) structures with complete and simultaneous photonic-phononic band gaps is still under serious consideration.¹⁶ On the other hand, the dielectric contrast required to open up an absolute photonic band gap is rather high (larger than five for the optimum geometries); therefore, the choice of metallic, instead of dielectric, inclusions offers an alternative route to design low-loss photonic nanostructures that exhibit sizeable and robust absolute gaps at near infrared and optical wavelengths.¹⁸ Any metal with relatively low absorption in this region, such as Au or Ag, would be appropriate for this purpose. Our goal in this letter, is to propose 3D metallodielectric phoxonic architectures with absolute spectral gaps. In particular, we demonstrate through rigorous multiple-scattering calculations that simple cubic (sc) lattices of metallic spheres with diameters close to half a micron, in an epoxy matrix, exhibit absolute band gaps for both light and sound. These features are scalable through a wide range of EM and sound frequencies but we have focused on structures with potential applications in telecommunications with optical band gap close to 1.5 μm and simultaneous acoustic band gap in the gigahertz range. Such structures can be realized in the laboratory using modern self-assembly nanofabrication techniques.

The multiple-scattering method that we use in the present study was developed both for electrostatics and elastodynamics and ignores any coupling between them. It relies on the same principles for both fields and has been discussed in detail elsewhere.^{19–21} In brief, the optical and elastic response of our structures is calculated following the methodology of the layer Koringa–Kohn–Rostoker method,¹

^{a)}Electronic mail: n.papanikolaou@imel.demokritos.gr.

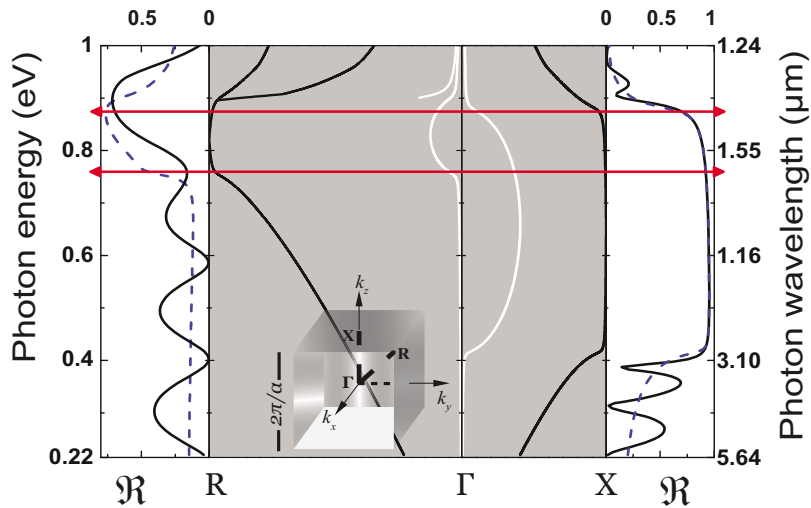


FIG. 1. (Color online) Complex photonic band structure and reflectance, \mathfrak{R} , of a sc crystal with lattice constant $a=480$ nm of Au spheres with diameter 460 nm in an epoxy matrix, along the ΓX and ΓR directions (see inset). The white lines show the imaginary part of the wave vector. The calculation was done with the experimental dielectric function of Au, which includes absorption. Next to the band diagrams we display the corresponding reflection spectra of (001) and (111) slabs of the crystal, five-layers thick, together with the reflectivity of the semi-infinite crystal (dashed lines). The extent of the absolute gap is marked by the horizontal lines.

where the crystal under study is decomposed into interacting successive layers with the same 2D periodicity, parallel to a given crystallographic plane. The method is ideally suited for layered structures of scatterers and, among its merits, it provides realistic scattering information for finite and semi-infinite slabs of a crystal, besides the complex band structure.

After carrying out systematic calculations for 3D crystals of metallic spheres in a dielectric host medium, for different materials and geometry, we deduced an optimized crystal that we consider here. It consists of Au spheres of diameter 460 nm arranged in a sc lattice, with lattice constant 480 nm, in a homogeneous epoxy matrix. The dielectric function of the Au spheres is obtained from the experimental optical data measured by Johnson and Christy,²² while a refractive index $n=1.6$ is used for epoxy. In Fig. 1, we display the complex photonic band structure of the given crystal along the directions ΓX and ΓR defined by the symmetry points of the bulk Brillouin zone (BZ) shown in the inset. The realistic complex permittivity of Au causes all bands to become complex, in the sense that all values of the wave vector acquire a small imaginary part to account for dissipative losses. To estimate the effect of absorption, we calculated the photonic bands by setting the imaginary part of the dielectric function of Au equal to zero.^{23,24} Our results justify the assumption of a low-loss photonic crystal around the telecommunication wavelength ($1.5 \mu\text{m}$), since the two calculations yield bands which are almost indistinguishable for most frequencies except near the edges of the band gap. The approximation of neglecting absorption turns out to work in defining the band gap²⁴ but one should be more careful for higher frequencies closer to the optical part of the spectrum. Here we stress that this approximation is a quick and efficient way to obtain a reliable description of the photonic bands of metallodielectric systems for Au and Ag, in the frequency region under consideration. However, such an approximation must be used with caution since it can fail for other metals with stronger absorption like Al. Absorption effects are more clearly manifested in the reflection spectra shown in Fig. 1, where the reflectivity is less than unity over the gap regions. Losses are more profound along the ΓR direction, but still the overall effect does not change the fact that the given crystal exhibits a full band gap with its lower edge at R and its upper edge at X, as we verified by detailed calculations. The center of the gap is around $1.55 \mu\text{m}$, extending from 1.41 to $1.64 \mu\text{m}$, while scaling to longer wave-

lengths is possible. In the gap regions, where there are no propagating Bloch modes, the attenuation is determined from the complex band of the proper symmetry which has the smallest in magnitude imaginary part. The reflectivity curves in Fig. 1 exhibit Fabry–Perot-type oscillations due to the multiple scattering between the surfaces of the slabs. These oscillations, of course, disappear in the limit of the semi-infinite crystal. The reflectivity associated with the (001) surface of the semi-infinite crystal, for normally incident light, approaches a value of about 0.95 in the gap region and is practically the same with that of a corresponding slab, five-layers thick. On the contrary, five (111) layers are not enough to approach the semi-infinite limit as shown in the reflectivity curves on the left of the band diagram. Our calculations show that at least eight layers are required in this case but the general conclusion is that absorption along any propagation direction is relatively small.

We now consider the elastodynamic response of the given crystal assuming the constituent materials to be elastically isotropic and lossless, which is a reasonably good approximation in our case. We use a mass density $\rho=19.3 \text{ g/cm}^3$ for Au, with the respective compressional and shear speed of sound to be $c_l=3376 \text{ m/s}$ and $c_t=1482 \text{ m/s}$. The epoxy matrix has $\rho=1.19 \text{ g/cm}^3$, $c_l=2860 \text{ m/s}$, and $c_t=1800 \text{ m/s}$. In Fig. 2, we show the frequency band structure of the acoustic field for the given crystal along the same directions as in the case of photonic bands (inset of Fig. 1). In the band diagram, one observes two following distinct families of bands: doubly degenerate bands, corresponding to shear waves, and nondegenerate ones, corresponding to either compressional or deaf modes.²⁵ Large hybridization gaps²⁶ are supported for both polarizations. In Fig. 2 the reflectance of slabs consisting of five (001) layers (right) and five (111) layers (left), for both shear and compressional incident waves, is shown next to the corresponding band diagram. The reflection spectra exhibit Fabry–Perot oscillations over the band regions and are practically unity in the gaps, the position of which changes only slightly as we scan different directions in the BZ. Although there is a secondary absolute frequency gap at higher frequencies, the gap edges at points Γ and R, 1.6 GHz and 2.8 GHz , respectively, define a large omnidirectional frequency gap of relative width 53.2%.

A systematic investigation of different cubic structures (sc, fcc, and bcc) of Au nanospheres in epoxy, by varying the

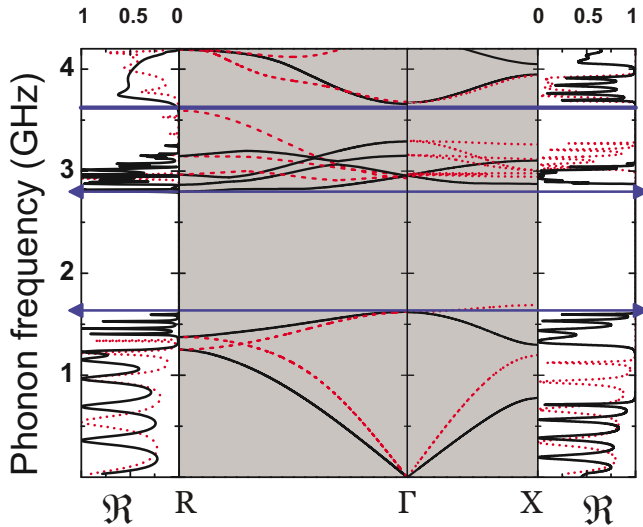


FIG. 2. (Color online) Phononic band structure and reflectance, \mathfrak{R} , of the crystal of Fig. 1 along the ΓX and ΓR directions (inset of Fig. 1). The solid and dashed lines represent doubly degenerate (shear) and nondegenerate (compressional or deaf) bands, respectively. Next to the band diagrams we display the corresponding reflection spectra of (001) and (111) slabs of the crystal, five-layers thick. Shear (compressional) waves correspond to solid (dashed) lines. The extent of the absolute gaps is marked by the horizontal lines.

lattice constant, reveals the existence of absolute phononic band gaps, in all three cases, over a broad range of volume filling fractions f . These gaps are wider for the more compact structures of large coordination number and increase with decreasing lattice constant to a maximum close to the touching-spheres limit, in agreement with previous studies on similar systems.²⁶ On the other hand, absolute photonic gaps open up only in the sc structure, above $f=40.3\%$, and their size increases with increasing volume filling fraction. This, of course, does not preclude the existence of simultaneous photonic and phononic band gaps in more complex structures like diamond or multicomponent systems with particles or voids of different sizes.

In conclusion, devices capable of integrating the management of heat, sound, and light simultaneously require the development of 3D phoxonic architectures, since 2D crystals can only partially control the above properties. Along this direction, assisted by rigorous full electrodynamic and elastodynamic multiple-scattering calculations, we propose a class of 3D metallodielectric phoxonic crystals. In particular, we demonstrated that a sc lattice of almost touching Au spheres with diameter of 460 nm in an epoxy matrix possesses sizeable absolute spectral gaps of relative widths 15.4% and 53.2% for EM and acoustic waves, respectively. The photonic gap extends about the 1.5 μm telecommunica-

tion wavelength, while losses in this spectral region are not severe to preclude applications in waveguiding and light localization in cavities. The phononic bands are fully scalable to any dimension while the basic features of the photonic bands can be scaled from microwave to optical wavelengths.

Financial support by FET-Open Project TAILPHOX (Grant No. 233883) is acknowledged.

¹A. Modinos, N. Stefanou, I. E. Psarobas, and V. Yannopoulos, *Physica B* **296**, 167 (2001).

²J. D. Joannopoulos, R. D. Meade, and J. N. Winn, *Photonic Crystals: Molding The Flow of Light* (Princeton University Press, New Jersey, 1995).

³*Photonic Crystals and Light Localization in the 21st Century*, edited by C. M. Soukoulis (Kluwer Academic, Dordrecht, 2001).

⁴M. Sigalas, M. S. Kushwaha, E. N. Economou, M. Kafesaki, I. E. Psarobas, and W. Steurer, *Z. Kristallogr.* **220**, 765 (2005).

⁵Z. Liu, X. Zhang, Y. Mao, Y. Y. Zhu, Z. Yang, C. T. Chan, and P. Sheng, *Science* **289**, 1734 (2000).

⁶W. Cheng, J. J. Wang, U. Jonas, G. Fytas, and N. Stefanou, *Nature Mater.* **5**, 830 (2006).

⁷T. Gorishnyy, J.-H. Jang, C. Koh, and E. L. Thomas, *Appl. Phys. Lett.* **91**, 121915 (2007).

⁸M. de Lima, Jr. and P. Santos, *Rep. Prog. Phys.* **68**, 1639 (2005).

⁹T. Gorishnyy, M. Maldovan, C. Ullal, and E. L. Thomas, *Physics World* **18**, 24 (2005).

¹⁰D. A. Mazurenko, X. Shan, J. C. P. Stiefelwagen, C. M. Graf, A. van Blaaderen, and J. I. Dijkhuis, *Phys. Rev. B* **75**, 161102 (2007).

¹¹A. V. Akimov, Y. Tanaka, A. B. Pevtsov, S. F. Kaplan, V. G. Golubev, S. Tamura, D. R. Yakovlev, and M. Bayer, *Phys. Rev. Lett.* **101**, 033902 (2008).

¹²K. Busch and S. John, *Phys. Rev. E* **58**, 3896 (1998).

¹³M. Eichenfield, J. Chan, R. M. Camacho, K. J. Vahala, and O. Painter, *Nature (London)* **462**, 78 (2009).

¹⁴M. Eichenfield, J. Chan, R. M. Camacho, K. J. Vahala, and O. Painter, *Nature (London)* **459**, 550 (2009).

¹⁵S. Sadat-Saleh, S. Benhabane, F. I. Baida, M.-P. Bernal, and V. Laude, *J. Appl. Phys.* **106**, 074912 (2009).

¹⁶M. Maldovan and E. L. Thomas, *Appl. Phys. B: Lasers Opt.* **83**, 595 (2006).

¹⁷M. Maldovan and E. L. Thomas, *Appl. Phys. Lett.* **88**, 251907 (2006).

¹⁸A. Moroz, *Phys. Rev. B* **66**, 115109 (2002).

¹⁹N. Stefanou, V. Yannopoulos, and A. Modinos, *Comput. Phys. Commun.* **113**, 49 (1998).

²⁰N. Stefanou, V. Yannopoulos, and A. Modinos, *Comput. Phys. Commun.* **132**, 189 (2000).

²¹R. Sainidou, N. Stefanou, I. E. Psarobas, and A. Modinos, *Comput. Phys. Commun.* **166**, 197 (2005).

²²P. B. Johnson and R. W. Christy, *Phys. Rev. B* **6**, 4370 (1972).

²³W. Y. Zhang, X. Y. Lei, Z. L. Wang, D. G. Zheng, W. Y. Tam, C. T. Chan, and P. Sheng, *Phys. Rev. Lett.* **84**, 2853 (2000).

²⁴S. Brand, R. A. Abram, and M. A. Kaliteevski, *Phys. Rev. B* **75**, 035102 (2007).

²⁵R. Sainidou, N. Stefanou, I. E. Psarobas, and A. Modinos, *Z. Kristallogr.* **220**, 848 (2005).

²⁶R. Sainidou, N. Stefanou, and A. Modinos, *Phys. Rev. B* **66**, 212301 (2002).